

Simulation and Experimental Studies of DWDM Nonlinear Phase/Polarization/Power Crosstalk Between DFOS and Communication Channels in 27.6-Tb/s 800ZR Metro Network

Jingchuan Wang⁽¹⁾, Maoqi Liu^(1,*), Liwang Lu⁽¹⁾, Alan Pak Tao Lau⁽¹⁾, Chao Lu⁽¹⁾

⁽¹⁾Photonics Research Institute, The Hong Kong Polytechnic University, Hong Kong SAR, China, jingchuan98.wang@connect.polyu.hk, maoqi.liu@connect.polyu.hk

Abstract We comprehensively analyze the fiber nonlinearity crosstalks between DAS and communication channels through numerical results and 40×800-Gb/s 90-km experimental demonstration. Our findings indicate that conventional pulse-based DAS is unsuitable for in-band DWDM coexistence system, whereas pulse-compression DAS shows negligible penalties with legacy coherent transceivers. ©2025 The Author(s)

Introduction

Future metro fiber networks will need real-time health monitoring, driving the development of integrated sensing and communication over fiber (ISACoF)^[1]. ITU-T recommends using 1625 nm or 1650 nm channels for in-service fiber monitoring^[2]. Recently, ITU-T SG15 has also explored the coexistence of distributed fiber-optic sensing (DFOS) and communication, particularly using dense wavelength division multiplexing (DWDM)^[3].

Several studies have explored the coexistence of distributed acoustic sensing (DAS) and communication data streams using WDM. Experiments inserting chirped-pulse DAS among 13 data wavelengths examined performance degradation in both co- and counter-propagation over 80 km fibers^[4]. Co-propagation of L-band DAS and 100-Gb/s coherent signals over 50 km showed no communication penalty with chirped-pulse DAS^[5]. The impact of stimulated Raman scattering between OTDR and other WDM channels suggests the need for pre-corrections in both OTDR and data channels^[6]. A field trial demonstrated real-time DAS and 400GbE coexistence, analyzing the tradeoff between DAS and data channel power^[7]. However, most prior work focuses on how much DAS degrades communication signals (e.g., BER or SNR), with little discussion on why and how DAS causes nonlinear crosstalk in legacy DWDM metro networks. Crucially, there is no systematic study on fiber nonlinearity crosstalk and tradeoffs needed before deploying DWDM ISAC networks.

This paper provides simulation and experimental analysis of fiber nonlinearity crosstalk between C-band 40λ × 800ZR data channels and a DAS channel over 90 km, focusing on nonlinear phase and polarization noise (PPN) and the Raman effect. Three key findings are highlighted: (1) For nearby data channels (<0.8 THz), high-peak-power DAS pulses can induce strong nonlinear birefringence, causing rapid polarization rotation—often a bigger issue than cross-phase

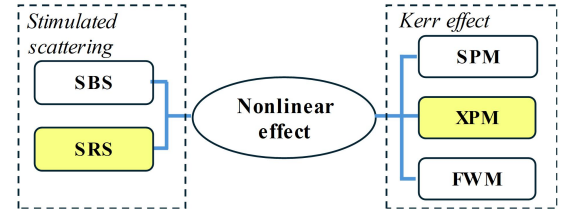


Fig. 1: Nonlinear effects in optical fibers.

modulation (XPM), as depolarization occurs before phase noise recovery in legacy transceivers. (2) For data channels farther from the DAS wavelength (>0.8 THz), the main coexistence problem is the stimulated Raman effect (SRS), especially in ZR (≥80 km) metro networks. The burst-like DAS pulses cause sudden power fluctuations in data channels, which can impact legacy amplifiers and receivers. (3) Pulse-compression-based DAS has minimal impact on data channels due to its low peak power and longer pulse duration.

Nonlinear effects in DWDM coexistence system

For metro link > 50 km, the nonlinear length is sufficient for averaging the rapid mixing of the polarization state on the Poincaré sphere^[8]. We have

$$\frac{\partial u}{\partial z} = -\frac{\alpha}{2}u - \frac{i\beta_2}{2}\frac{\partial^2 u}{\partial t^2} + i \cdot \frac{8}{9}\gamma \left[(1 - f_R) ||u||^2 u + f_R \cdot u \int_{-\infty}^{\infty} h_R(\tau) (||u(t - \tau)||^2) d\tau \right], \quad (1)$$

where $u(z, t)$ denotes E_x or E_y polarizations, β_2 , γ , f_R and h_R are the group velocity dispersion and nonlinear parameter, Raman contribution factor and response function. Fiber nonlinearities are concluded in Fig. 1, where highlighted blocks are the main nonlinear impacts induced by the DAS pulse. Because the minimum granularity of flex-grid DWDM is 12.5 GHz, the crosstalk by stimulated Brillouin scattering (SBS) can be ignored with the properties of narrow-band gain and typical 11.8 GHz Brillouin frequency shift (BFS).

Fig. 2(a) and (b) show conventional pulse-based DAS and linear frequency-modulated (LFM) pulse-

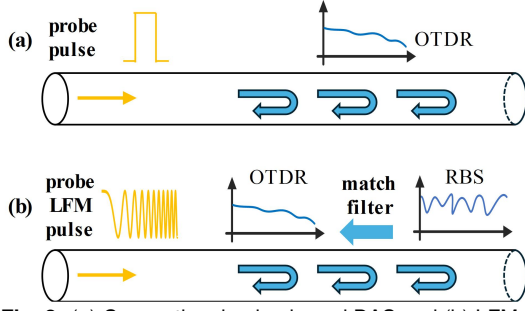


Fig. 2: (a) Conventional pulse-based DAS and (b) LFM pulse-compression DAS

compression DAS schemes. Conventional pulse-based DAS cannot cover ZR distances (≥ 80 km) without heavy averaging or Raman amplification, so two bidirectional interrogators are needed for the 90-km fiber in our experiment. In contrast, LFM pulse-compression DAS, with longer pulses and matched filtering, can monitor up to 100 km^[9], meeting 800ZR requirements. Also, conventional DAS needs much higher peak power for long distances, greatly increasing nonlinear crosstalk to other channels.

Tab. 1: Numerical simulation parameters

Parameter	Value
Fiber length	90 km G.652D
DAS channel	C34
Data channels	C21-C33 & C35-C61
PMD coefficient	0.1 ps/ \sqrt{km}
Raman factor	18 %
Raman response time	3 fs
Data per channel	0 dBm 80 GBaud
DAS pulse duration	500 ns
Pulse rise/fall time	50 ns
Peak power of DAS	17-21 dBm
SSFM stepsize	5 m

We use the Manakov Equation (Eq. 1) to simulate 90 km fiber coexistence between a pulse-based DAS channel at C34 and ITU-T C21–C61 communication channels (specifications in Table 1). All other channels transmit 80 GBaud QPSK data. To allow DAS interrogation from both ends over 50 km, we set a 500 ns pulse width and vary the peak power from 17 to 21 dBm—levels chosen to approach, but not cause, significant nonlinear effects^[10]. The DAS pulses also have 50 ns rise/fall edges, matching commercial systems. For data channels more than 0.8 THz from the DAS channel in co-propagation, Fig. 3 shows power fluctuations in data frames overlapping with pulses, caused by the Raman effect. Fig. 4a shows that adjacent channels (<0.8 THz) experience burst signal slips during the DAS pulse edges. In counter-propagation, data channels are unaffected. Fig. 4b also shows diffused constellation points during rise/fall edges, confirming pulse-induced distortions from nonlinear polarization and XPM noise.

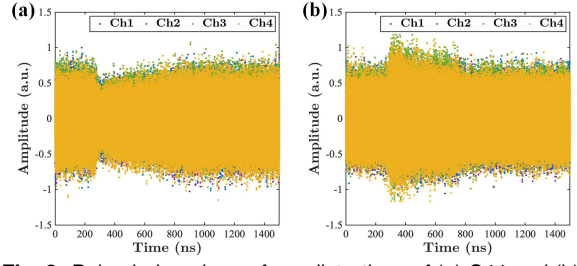


Fig. 3: Pulse-induced waveform distortions of (a) C44 and (b) C24, burst power-fluctuating due to Raman effect.

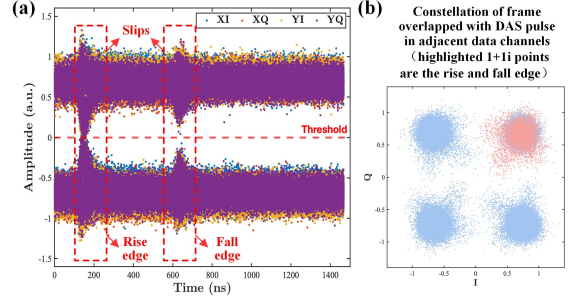


Fig. 4: (a) Decoded data (C34) in 20 dBm peak power pulse (C33). (b) Constellation with rise/fall time highlighted.

Experimental setup and result discussions

Coexistence experiment of 90 km $40\lambda \times 80$ GBaud 32/16/4-QAM channels and 1λ DAS channel is consistent with numerical simulation. Both co-propagation and counter-propagation experiments are done, with only co-propagation case depicted in Fig. 5a. We slide the wavelength of integrated tunable laser assembly (ITLA) to test the communication performance of each channel, while other data channels are loaded with amplified spontaneous emission (ASE) noise at same power level. Dummy band is generated by a C-band ASE source and shaped by a wavelength selective switch (WSS, Finisar 4000A). Communication setup consists of 120 GSa/s arbitrary waveform generator (AWG, Keysight 8194) and 256 GSa/s real-time oscilloscope (RTO UXR0804). Sensing includes narrow linewidth laser (NLL, NKT X15) and acousto-optic modulator (AOM, G&H) for generating pulse of 500 ns or LFM-pulse of 5000 ns and 15 MHz sweeping bandwidth. A 60 m piezoelectric transducer (PZT) acts as a vibrator between two fiber spools. An integrated coherent receiver (ICR, Lumentum Class 40) and 20 GSa/s scope (Keysight, MSOS404A) are used to receive the Rayleigh backscattering signal (RBS).

Tab. 2: Raman effect induced burst power fluctuation. Define power variation exceeding 20% of the average as fail.

Pulse cases	Remark
peak power > 19 dBm, C21-C25	fail
peak power > 19 dBm, C43-C61	fail
C26-C33 & C35-C42	pass
LFM-pulse cases (C21-C61)	Remark
No fluctuations under peak power < 13 dBm	

We analyze the Raman effect for co-propagation cases, with pulse and LFM-pulse results shown

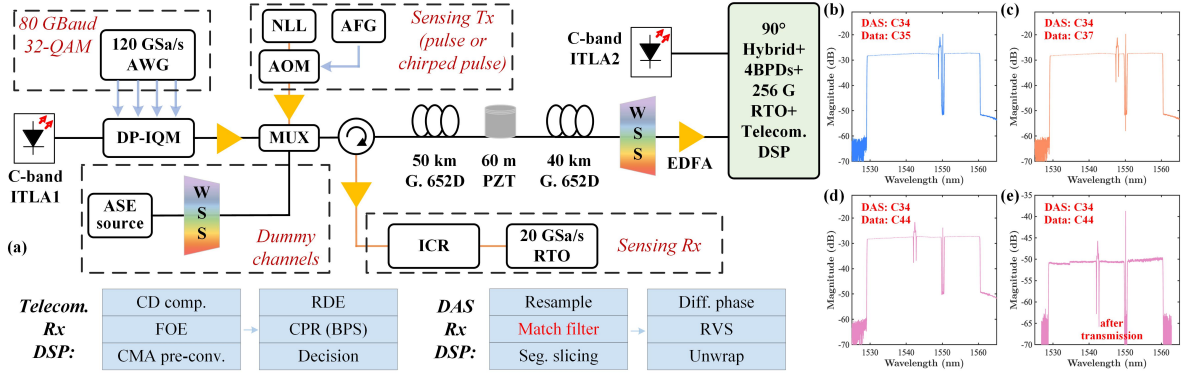


Fig. 5: (a) Experimental setup of co-propagating case. (b)-(e) Spectrum of testing data channels, co-propagating with pulse.

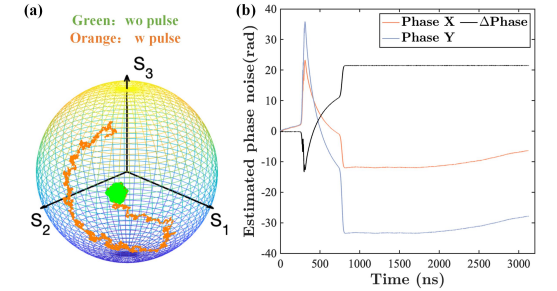


Fig. 6: (a) Poincaré sphere from taps. (b) Phase noise plot.

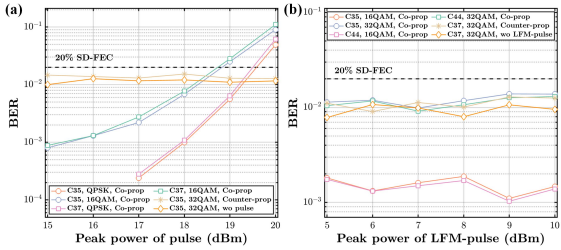


Fig. 7: (a) BER with pulse. (b) BER with LFM-pulse.

in Table 2. Practically, burst power fluctuation exceeding the threshold will cause additional penalty to legacy amplifiers and ZR transceivers.

Then we investigate the nonlinear polarization and phase noise of the adjacent channels (C26-C32 & C35-C42). The Stokes parameters of polarization are obtained by equalization taps^[11]. Fig. 6a indicates a burst polarization rotation over the pulse duration when peak power exceeds 17 dBm. Fig. 6b also reveals that different XPM-induced phase noise is observed of two polarizations with pulse on. These findings support that both nonlinear polarization and phase noise exist in the co-existence system due to the polarization misalignment of pulse and data. Furthermore, once we can successfully track the polarization change in the experiment, we can recover the XPM-induced phase noise, suggesting the former effect may be the main constraint of coexistence system.

To analyze the communication performance, we set the launch power of each data channel to be 0 dBm and scan the peak power of the co-propagation pulse from 15 dBm to 20 dBm. Fig. 7a shows a sharp degradation of bit error rate (BER) as the peak power increases both in the 1st and 3rd adjacent channels. In contrast, neg-

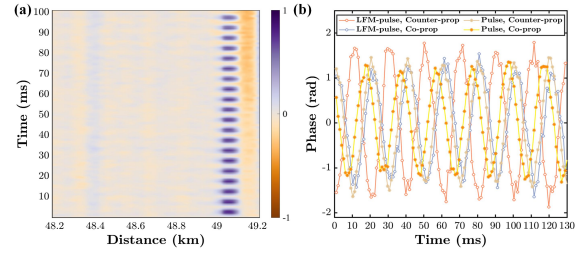


Fig. 8: (a) Waterfall plot. (b) Demodulated vibrations.

ligible penalties are observed when data channels transmit accompanied with LFM-pulse from 5 dBm to 10 dBm, as shown in Fig. 7b. Considering 16.7% overhead of SD-FEC, we achieve $40 \times 800\text{G} \times 83\% = 26.7\text{ Tb/s}$ ZR transmission.

Pulse (peak power 15-20 dBm) and LFM-pulse (peak power 5-10 dBm) reaches the similar SNR of DAS traces, while LFM-pulse can achieve finer sensing resolution. As pulse setup is hard to cover 90 km fiber without fadings, we need to do both co-propagation and counter-propagation from both sides. Fig. 8a is the demodulated waterfall plot of 200 Hz vibration, interrogated by the co-propagation LFM pulse. Also, a 50 Hz vibration is successfully detected via co-/counter-propagation and pulse/LFM-pulse, shown in Fig. 8b.

Conclusion

We studied the in-band nonlinear crosstalks from conventional pulse-based and pulse-compression based DFOS in 800GZR metro networks. For data channels over 0.8 THz from the DAS channel (co-propagation), the main issue of coexistence is SRS-induced power fluctuation. For channels within 0.8 THz, nonlinear polarization rotation may have more severe impact on legacy coherent transceivers, compared with XPM-induced phase noise. Counter-propagating DAS causes little penalty to data channels, but one-side DAS cannot cover ZR distances. Besides, pulse-compression based DAS is highlighted for negligible nonlinear penalty to data channels and the ability to fully cover ZR distances. These findings on the nonlinear mechanisms and tradeoffs between sensing and communications will help guide future DFOS and high-speed communication coexistence design and standards.

Acknowledgements

This work is supported by the Hong Kong Research Grants Council (GRF 15227321, GRF 15225423) and Hong Kong Polytechnic University project 1-CD8L. We would like to acknowledge the contributions from Dr. Qirui Fan and Mr. Chuang Xu.

References

- [1] M.-F. Huang, M. Salemi, Y. Chen, *et al.*, “First field trial of distributed fiber optical sensing and high-speed communication over an operational telecom network”, *Journal of Lightwave Technology*, vol. 38, no. 1, pp. 75–81, 2019.
- [2] ITU-T, *G.697: Optical monitoring for dense wavelength division multiplexing systems*.
- [3] ITU-T SG15, *ITU Workshop on ‘Evolution of Optical Networks for IMT2030 and Beyond’*. Hong Kong, 20 November 2024.
- [4] Z. Jia, L. A. Campos, M. Xu, *et al.*, “Experimental co-existence investigation of distributed acoustic sensing and coherent communication systems”, in *2021 Optical Fiber Communications Conference and Exhibition (OFC)*, IEEE, 2021, pp. 1–3.
- [5] L. Shen, W. Yu, R. Xu, Y. Wang, and B. Du, “Co-propagation of distributed acoustic sensing in the l-band and 100-gb/s wdm coherent communication systems”, in *2022 Asia Communications and Photonics Conference (ACP)*, IEEE, 2022, pp. 629–632.
- [6] C. Zhang, X. Liu, J. Li, *et al.*, “Optical layer impairments and their mitigation in c+ l+ s+ e+ o multi-band optical networks with g. 652 and loss-minimized g. 654 fibers”, *Journal of Lightwave Technology*, vol. 40, no. 11, pp. 3415–3424, 2022.
- [7] Y.-K. Huang, Z. Wang, E. Ip, *et al.*, “Field trial of coexistence and simultaneous switching of real-time fiber sensing and 400gbe supporting dci and 5g mobile services”, in *2023 Optical Fiber Communications Conference and Exhibition (OFC)*, IEEE, 2023, pp. 1–3.
- [8] P.-K. A. Wai, C. R. Menyuk, and H. H. Chen, “Stability of solitons in randomly varying birefringent fibers”, *Optics letters*, vol. 16, no. 16, pp. 1231–1233, 1991.
- [9] M. R. Fernández-Ruiz, L. Costa, and H. F. Martins, “Distributed acoustic sensing using chirped-pulse phase-sensitive otdr technology”, *Sensors*, vol. 19, no. 20, p. 4368, 2019.
- [10] H. F. Martins, S. Martin-Lopez, P. Corredera, P. Salgado, O. Frazão, and M. González-Herráez, “Modulation instability-induced fading in phase-sensitive optical time-domain reflectometry”, *Optics letters*, vol. 38, no. 6, pp. 872–874, 2013.
- [11] J. Wang, M. Liu, J. Zhang, L. Lu, A. P. Tao Lau, and C. Lu, “Forward polarization sensing triggered area-focus das over a bidirectional coherent network”, *Optics Letters*, vol. 50, no. 7, pp. 2227–2230, 2025.